# A simulation chain for reflectometry and non-linear MHD: Type-I ELM case

**J. Vicente,[a,1] F. da Silva,[a] M. Hoelzl,[b] G. D. Conway,[b] and S. Heuraux [c]**

[a] *Instituto de Plasmas e Fusão Nuclear, Instituto Superior Técnico, Universidade de Lisboa, 1049-001 Lisboa, Portugal*

[b] *Max-Planck-Institut für Plasmaphysik, 85748 Garching, Germany*

[c] *Institut Jean Lamour, University of Lorraine-CNRS, F-54011 Nancy, France*

*E-mail*: jvicente@ipfn.tecnico.ulisboa.pt

ABSTRACT: A complete chain from a non-linear MHD plasma model simulation through full-wave code simulations implementing synthetic conventional reflectometry is established. For this purpose, the two-dimensional full-wave code REFMUL is employed together with MHD descriptions obtained from the JOREK code. First results of the integrated modeling are presented here where a Type-I ELM crash, leading to a fast collapse of the H-mode pedestal, was taken as case-study. The REFMUL simulations were customized to implement synthetic reflectometry in conventional set-up using fixed frequency probing with O-mode waves. Posing challenging conditions for reflectometry, the Type-I ELM crash reveals some of the merits and caveats of the diagnostic technique. This work also opens up the possibility to extend modeling to other MHD or ELM studies and provide support to experimental observations with reflectometry.

KEYWORDS: Modelling of microwave systems; Nuclear instruments and methods for hot plasma diagnostics; Simulation methods and programs.

[1] Corresponding author.

## Contents



## 1. Introduction

The development of magneto-hydrodynamic (MHD) instabilities determines to a great extent the properties of magnetized plasmas as well as the viability of plasma scenarios for future fusion devices. On the modelling side, the evolution of non-linear MHD instabilities is anticipated with increasing accuracy through codes such as JOREK [1,2]. JOREK allows to study large-scale MHD instabilities in tokamak configurations with X-point plasmas covering the main plasma, the scrape-off layer (SOL) and the divertor regions. JOREK non-linear simulations are able, for example, to investigate the underlying non-linear physics of Edge Localized Modes (ELMs) driven by large pressure gradients and current densities at the edge of H-mode plasmas. This includes the study of ELM crashes, ELM-free regimes, ELM pacing by pellets and magnetic kicks, and mitigation or suppression by resonant magnetic perturbation coils (RMPs). On the other hand, microwave reflectometry is an established experimental technique that has been applied to measure electron density fluctuations and profiles among other plasma parameters (e.g. see [3]). Reflectometry is thus an experimental diagnostic that has been used to characterize turbulence and MHD, while it has also found strong support in modeling activities to provide quantitative data interpretation.

In this work, a simulation chain was built that allows to easily implement synthetic reflectometry diagnostics in order to simulate MHD measurements with realistic plasma models. For that purpose, outputs obtained from the non-linear MHD code JOREK were integrated into the two-dimensional full-wave code REFMUL [4] which is a well-established reflectometry code. To demonstrate the integrated modeling capabilities, the JOREK simulation of a typical Type-I ELM crash was taken as case study. A JOREK simulation that has been previously treated and well characterized in literature was chosen [5,6]. It was also taken into account that this case study was based on the characteristics of an ELM cycle observed during a plasma discharge at the ASDEX Upgrade (AUG) tokamak where an experimental ordinary mode (O-mode) reflectometry system can be used as reference for the synthetic diagnostic that was implemented [7,8].

## 2. Synthetic reflectometry

The working principles of reflectometry are radar-like, based on time of flight or phase measurements of electromagnetic waves that are used to probe fusion plasmas. Depending on

different assumptions and approximations, one of several relations between phase fluctuations $\delta\varphi$ and electron density perturbations $\delta n_e$ can be derived (e.g. see [9]). Thus, phase measurements obtained with fixed frequency probing waves are usually devoted to measure density fluctuations. In the case of O-mode, waves are reflected at the critical electron density $n_c = f_o^2(4\pi^2\varepsilon_o m_e/e^2)$ where $f_o$ is the probing frequency, $e$ and $m_e$ the electron charge and mass, and $\varepsilon_o$ the permittivity of free space.

The REFMUL code solves the Maxwell equations for O-mode in 2D on two staggered Cartesian grids, using the finite-difference time-domain (FDTD) technique. The electric and magnetic fields are coupled to the electron density through the current density equation. The electron density is in fact the only plasma parameter required to describe the plasma in this model. The Cartesian grids follow a spatial discretization $\Delta x = \Delta y = 3.75 \times 10^{-4} m$ which is a small fraction of the probing wavelengths, where $x$ and $y$ correspond to the radial and poloidal directions in a tokamak. To ensure numerical stability, the time discretization must comply with the Courant-Friedrichs-Lewy (CFL) condition, which sets $\Delta t = 6.25 \times 10^{-13} s$. For the implementation of the synthetic reflectometer, the Unidirectional Transparent Source (UTS) technique is also employed to separate emission and reception. The synthetic diagnostic was implemented operating in fixed frequency, at either $f_o$ = 24 GHz or $f_o$ = 36 GHz similarly as in the experiment. Other characteristics of the AUG reflectometer, used as reference, determined the implementation of normal incidence (at the mid-plane of the low magnetic field side), a monostatic set-up with an H-plane horn antenna, a vacuum distance of around 22 cm from the antenna mouth to the plasma entry, and beam width at half-power ≤ 5.9cm (24 GHz) or ≤ 5.2cm (36 GHz) estimated from the radiation diagram in vacuum, at the plasma cut-off distance.

To obtain the in-phase and quadrature (I/Q) signals, as well as the reflectometer amplitude $A(t)$ and phase $\varphi(t)$ response from the REFMUL simulations, a method that is described in previous work was also employed here [10]. This method relies on considering the plasma frozen in the time scale of the probing wave. In fact, the time discretization employed in JOREK is usually several orders larger than in REFMUL. Thus, the approximation is valid and each plasma "snapshot" obtained from JOREK can be probed until a stationary response is obtained in REFMUL runs.

## 3. Coupling of JOREK and REFMUL codes

JOREK is a fully implicit non-linear extended MHD code that has become widely used to study large-scale plasma instabilities in realistic tokamak geometries. For a comprehensive review of the code details and capabilities, please see [2]. To integrate JOREK and REFMUL a set of requirements must be met while a few features also require some attention. A cylindrical coordinate system is used in JOREK that allows for flux-surface aligned iso-parametric finite element grids. The poloidal plane is discretized with 2D Bezier finite elements. Inside each of the finite elements another local coordinate system is employed. The first requirement to meet is the REFMUL spatial resolution. For that purpose, the JOREK data can be simply extracted by evaluating the finite element basis on the requested Cartesian grid positions.

JOREK also uses a fully implicit time stepping and an iterative solver. When the dynamics become very non-linear, the preconditioner is less accurate and convergence deteriorates such that the time step needs to be reduced. This results in non-regular time sampling of JOREK plasma quantities. For the REFMUL simulations, this is not taken into account before the $I(t)$, $Q(t)$, $A(t)$ and $\varphi(t)$ signals are reconstructed. It is only after obtaining the synthetic reflectometry

signals that these are interpolated into a regular time series, for instance prior to any spectral analysis of the signals.

According to the method used to reconstruct the I/Q time series, from the REFMUL simulations, reflectometry responses must be obtained for both the fully perturbed plasma $n_e(x,y) = n_{e0}(x,y) + \delta n_e(x,y)$ and the background (or base) plasma $n_{e0}(x,y)$ at each time instance [10]. While JOREK provides directly the data of total electron density, the background base plasma $n_{e0}(x,y)$ is computed in this work by point-wise averaging over 40 time-neighboring density maps obtained from JOREK. The variable time stepping used in JOREK implies that this averaging does not correspond to a constant time value, but to averaging in a range of [0.15 - 0.5] ms, depending on the ELM dynamics.

Regarding the size of the poloidal cross-section, it is usually sufficient to use a smaller Region of Interest (ROI) rather than the whole JOREK domain for the REFMUL simulations. In the left panel of Fig. 1 the actual ROI used in this work in the selected poloidal plane is shown. The JOREK data is retrieved in the equatorial LFS, bounded by the AUG cylindrical coordinate values $Z$ = [-0.1, 0.1] m, and $R$ = [2.12, 2.17] m. This ROI corresponds to a 2D Cartesian grid of 135×535 points using the required REFMUL spatial resolution. Note that the real aspect ratio was not kept in Fig. 1. It can also be seen from this figure that the Cartesian grid can be incomplete, if some Cartesian grid points are outside of the JOREK domain. In addition, the JOREK density data at the boundary of the JOREK domain does not vanishes completely but has some finite minimum value. Both kinds of abrupt changes in the medium could result in artificial phase jumps as waves propagate from the vacuum to the plasma and back. To overcome this issue, an exponential decay of the plasma density is included from each outer point of the radial density profiles using an additional extension of 80 grid points in the radial direction. This is also displayed in Fig. 1, on the right panel, where the density profile at the middle poloidal position is shown after pre-processing JOREK data for REFMUL integration. It should be noted that the data is reversed in the radial direction and that perfectly matched layers (PML) are used for optimized boundary conditions at the edge of the simulation grid. An average radial profile computed as discussed previously ($\overline{n_e} = n_{e0}$) is also displayed together with the corresponding critical density layers of the probing frequencies that were employed in this work.

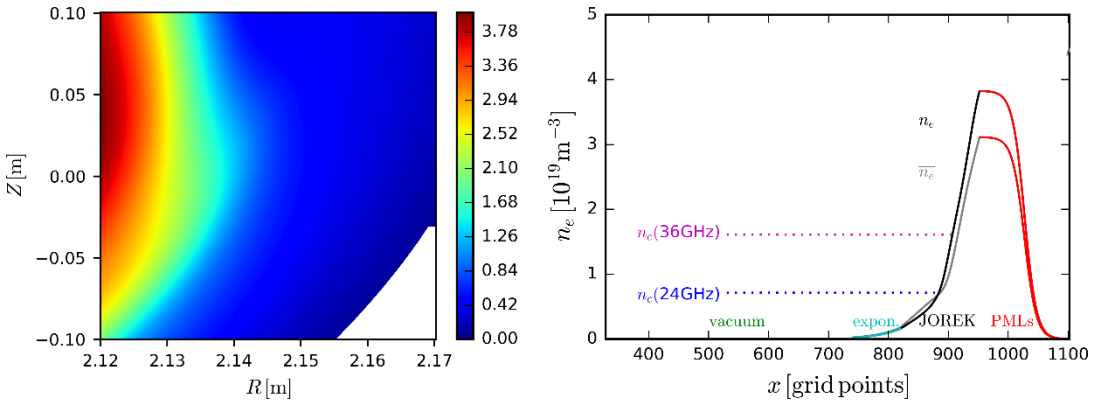


**Figure 1.** Left: Example of electron density map obtained directly from JOREK on the selected ROI of the poloidal plane. Right: Part of radial cut on data processed for REFMUL integration showing regions of vacuum, exponential decay, JOREK data itself ($n_e$) and PMLs. Data for the computed background plasma $\overline{n_e}$ is also shown where critical density layers for two probing frequencies are indicated.

## 4. The Type-I ELM case

The non-linear development of a single Type-I ELM has been simulated with JOREK. The simulation was based on the typical kinetic profiles measured experimentally, just before the ELM crash, on the peeling-ballooning unstable discharge #33616 on AUG at $t$=7.2s. Details on the simulation and experimental analysis can be found, in [5] and [6], respectively. The ELM crash obtained with the simulation occurs in a time period of about 2 ms, leading to a thermal energy loss of about 2.5% and to 7% of particles being lost across the separatrix. The duration of the ELM crash and particle losses display a good agreement with the several ELM cycles that were considered experimentally. Additional simulations with fully realistic parallel heat conductivity resulted in thermal energy losses of 7-8% more consistent with experimental observations [2]. However, a direct comparison with experiments is not envisaged in this work, for which the original simulation treated here will be sufficient. It is also important to note that the inter-ELM phases have not been investigated with this simulation.

The time interval of the JOREK simulation that was considered here (-0.25 ms < $t$-$t_{\mathrm{ELM}}$ < +2.50 ms, using the ELM onset time $t_{\mathrm{ELM}}$ as reference) corresponds to about 1130 *snapshots* of density maps. The spatial structure of the ELM shows that toroidal mode numbers $n$ = 3-5 are dominant during the crash, which is in good agreement with experimental observations. Density structures observed in the LFS mid-plane appear to move upwards, in the electron diamagnetic drift direction. The average amplitude of density structures evolving during the ELM is in the range of 5-30% according to Fig. 2 where the average $\langle \delta n_e/n_e \rangle$ profile is shown (red curve) as computed directly from the JOREK data along the whole ELM crash period at the antenna on-axis line of sight. The average density perturbation level displays one maximum inside the separatrix. Using the average density profile (black curve) to locate the radial position of critical density layers, it is found that for the probing frequencies $f_o$ = 24 GHz and $f_o$ = 36 GHz the average perturbation levels at the corresponding cut-off layers ($n_c = 0.71 \times 10^{19}\mathrm{m}^{-3}$ and $n_c = 1.61 \times 10^{19}\mathrm{m}^{-3}$, respectively) are of 18% and 27%. Note that individual density structures may display local $\delta n_e/n_e$ levels over 100%.

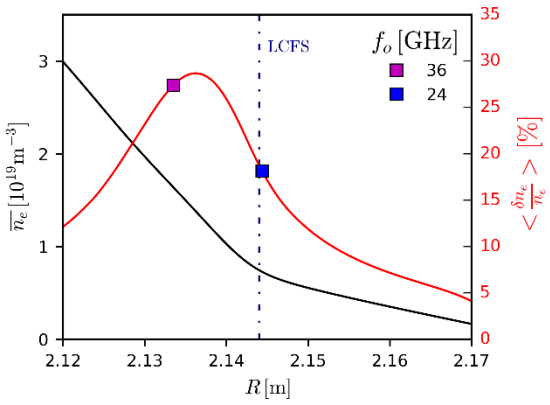


**Figure 2.** Average density profile (black) and average density perturbation level profile (red) computed at the central axis of the antenna using the full set of the ELM crash data. Perturbation levels at the radial locations of the corresponding critical density layers of selected probing frequencies are marked.

The evolution of the radial position and of the local density gradient length ($L_n$) at the cut-off density layers is shown in Fig. 3.

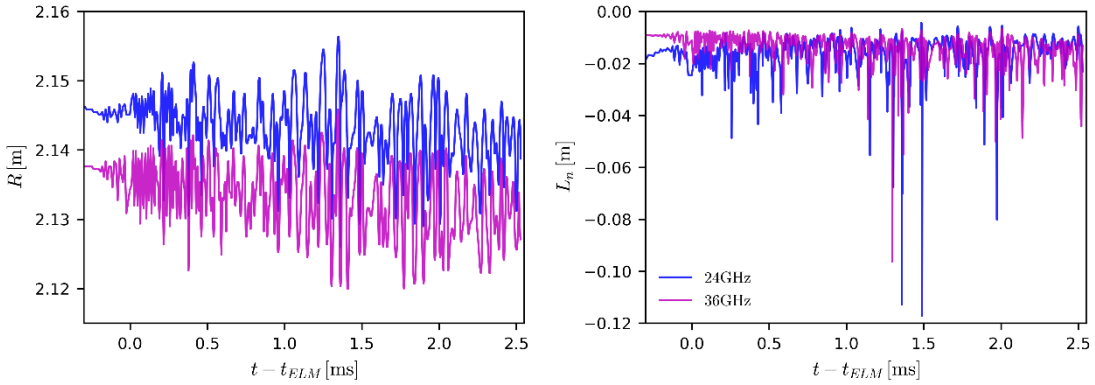


**Figure 3.** Evolution of radial displacement (left) and density gradient length (right) at the cut-off critical density layers of selected probing frequencies.

164

165 The behavior of both parameters is somewhat similar for the two probing frequencies, with
166 a fast development of intermittent radial displacements of the order of 1cm and the existence of
167 periods where the gradients become much more shallow indicated by longer density gradient
168 lengths.

169 Having looked at the ELM evolution directly from JOREK data, REFMUL simulations were
170 then run independently for each density map obtained from JOREK, according to the method
171 previously mentioned [10]. Each REFMUL run consisted of 120 thousand time-iteration points.
172 Reflectometry time sequences were then built subsequently by sampling each REFMUL output
173 data at the 90.000$^{th}$ iteration point, well into the stationary response regimes established at each
174 REFMUL run. Two different sets of REFMUL simulations were performed, considering the
175 operation of the synthetic diagnostic at $f_o$ = 24 GHz and $f_o$ = 36 GHz. The I/Q reflectometry data
176 reconstructed from REFMUL simulations are displayed in Fig. 4. The I/Q plots display a large
177 scatter in the data, together with large amplitude variations. It is thus not surprising that after
178 reconstructing the corresponding phase signals, rapid variations and phase runaway effects are
179 observed, as displayed in Fig. 5.

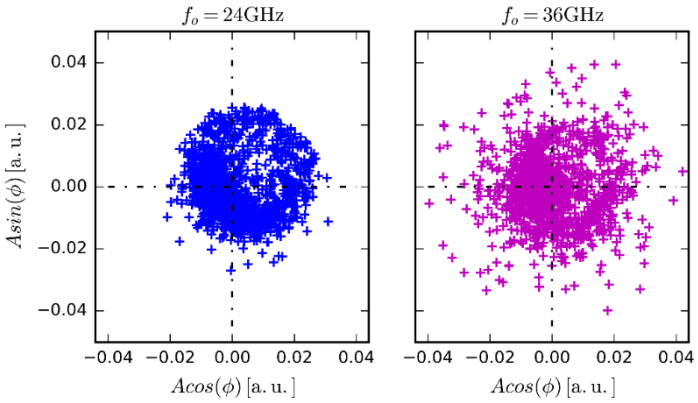


**Figure 4.** Scatter plot of synthetic reflectometry I/Q signals during the Type-I ELM crash for cases of $f_o$ = 24 GHz and $f_o$ = 36 GHz probing frequencies.

180

181

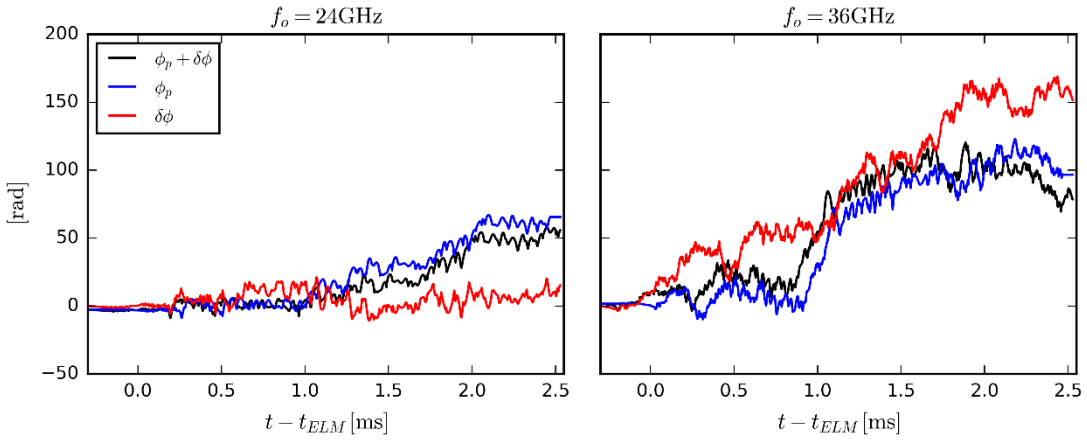


**Figure 5.** Time traces of synthetic reflectometry phase signals during the Type-I ELM crash for cases of $f_o$ = 24 GHz and $f_o$ = 36 GHz probing frequencies. The full reconstructed phase is shown along with the phase perturbation $\delta\varphi(t)$ and background $\varphi_p(t)$ components.

The distributions of phase increments, ranging between -$\pi$ and +$\pi$ between consecutive time samples, obtained from the same set of phase signals are also displayed in Fig. 6.

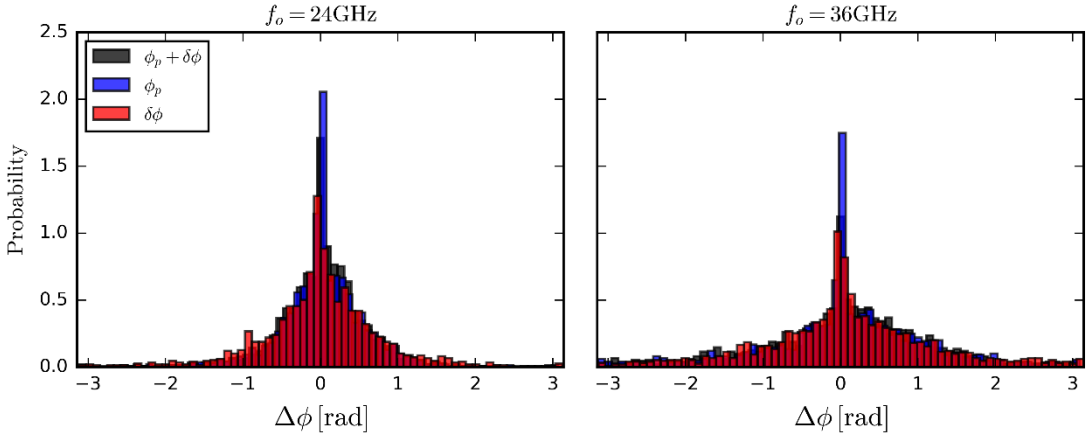


**Figure 6.** Histograms of phase increments from synthetic reflectometry during the Type-I ELM crash for cases of $f_o$ = 24 GHz and $f_o$ = 36 GHz probing frequencies.

The time traces of reconstructed reflectometry signals reveal that detrimental effects on the phase occur earlier and are more severe for the case of $f_o$ = 36 GHz probing frequency. In this case, the consecutive phase variations also display a broader distribution, of higher kurtosis, where large phase increments becoming more likely than in the lowest probing frequency case. This is likely related to the fact that at the corresponding critical density layers the perturbations are of larger amplitude for $f_o$ = 36 GHz, as it was previously shown in Fig. 2.

This phase behavior is typical of non-linear regimes of reflectometry, in particular when moderate to high turbulence levels are considered in the conventional set-up [11]. In this case, phase runaway effects are observed in both $\delta\varphi(t)$ and $\varphi_p(t)$ corresponding to density perturbations and unperturbed density profile contributions, respectively. The latter might be

related to large scale structures that remain important even after the averaging performed to obtain the background density data. Nevertheless, the phase artifacts seem uncorrelated with the local changes in the gradient scale length shown previously in Fig. 3. The data suggests that non-linearity occurs due to the large amplitude of density structures evolving during the ELM crash, similarly to what is expected from high turbulence levels [12].

A spectral analysis comparison can also be made between the REFMUL reflectometry signals and the time evolution of the electron density obtained directly from JOREK data at the radial location of the corresponding critical layers. While remaining a simplified treatment, instead of taking a point-wise observation, estimated spot sizes were considered to obtain the time evolution $\langle n_e \rangle(t)$ by spatial averaging JOREK data over the area of a given spot size. Different spectra obtained from REFMUL synthetic homodyne data and JOREK data, are shown in Fig. 7 where the frequency axis has been normalized using the sampling frequency $f_s$=595 kHz employed to interpolate the irregular time series.

The REFMUL spectra are broad and flat in the low frequency range (i.e. large scales) which is a characteristic of experimental observations with different diagnostics (reflectometry and magnetics, for instance) during ELM crashes. The spectra of $\langle n_e \rangle(t)$ obtained directly from JOREK reveals some structure which is not recovered by the synthetic diagnostic.

REFMUL spectra rolls-over above a given frequency value, as in the case of JOREK, with approximately constant slope or spectral index. It appears that for the case of $f_o$ = 36 GHz the "knee" occurs at a higher value, which is not evident from JOREK data. However, it does appear that the spectral content of the JOREK data has higher power in this range, than in the case corresponding to $f_o$ = 24 GHz. This also seems to be the case for REFMUL data. Hence, despite the likely saturated regime occurring in the low frequency range, which may be unpractical, the diagnostic appears to still retain some sensitivity at higher frequencies.

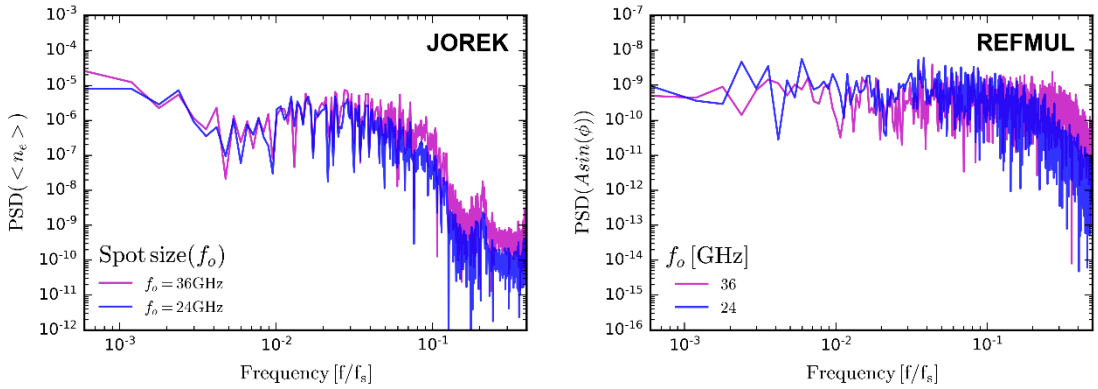


**Figure 7.** Left: Spectra of $\langle n_e \rangle(t)$ computed directly from JOREK data using critical layer and spot size information of $f_o$ = 24 GHz and $f_o$ = 36 GHz probing frequencies. Right: Spectra of the corresponding synthetic reflectometry quadrature (Q) signals obtained from REFMUL simulations.

## 5. Conclusions

A workflow to carry out full-wave simulations using the REFMUL code and JOREK non-linear MHD simulations has been successfully established. A Type-I ELM crash simulation obtained from JOREK, reproducing experimental conditions at the ASDEX Upgrade tokamak, was considered for the first case study of REFMUL simulations with integrated JOREK data. The Type-I ELM crash offers challenging conditions for reflectometry, displaying average density

perturbation levels of up to 30%. Reflectometry signals were retrieved displaying strong spectral broadening and phase runaway effects, as typically observed with experimental diagnostics. This work opens up the possibility to extend the understanding of MHD phenomena to other ELM studies (e.g. inter-ELM phases) using a complete chain from non-linear MHD to full-wave simulations of synthetic reflectometry.

## Acknowledgments

This work has been carried out partially within the framework of the French Federation for Magnetic Fusion Studies (FR-FCM). IST activities also received financial support from "Fundação para a Ciência e Tecnologia" through Scientific Employment Stimulus program and projects UIDB/50010/2020 and UIDP/50010/2020.

## References

[1] G.T.A. Huysmans and O. Czarny, *MHD stability in X-point geometry: simulation of ELMs*, *Nucl. Fusion* **47** (2007) 659

[2] M. Hoelzl, G.T.A. Huijsmans et al., *The JOREK non-linear extended MHD code and applications to large-scale instabilities and their control in magnetically confined fusion plasmas*, *Nucl. Fusion* **61** (2021) 065001

[3] G. D. Conway, *Microwave reflectometry for fusion plasma diagnosis,* Nucl. Fusion **46** (2006) S665

[4] F. da Silva et al., *Unidirectional transparent signal injection in finite-difference time-domain electromagnetic codes –application to reflectometry simulations, Journal of Comp. Physics* **203** (2005) 467-492

[5] M. Hoelzl et al., *Insights into type-I ELMs and ELM control methods from JOREK MHD simulations*, *Cont. to Plasma Phys.* **58** (2018) 518– 528

[6] A. F. Mink et al., *Nonlinear coupling induced toroidal structure of edge localized modes*, *Nucl. Fusion* **58** (2018) 026011

[7] L. Cupido et al., *Frequency hopping millimeter-wave reflectometry in ASDEX upgrade, Rev. Sci. Instrum.* **77** (2006) 10E915

[8] J. Vicente et al., *Synthetic conventional reflectometry probing of edge and scrape-off layer plasma turbulence*, *JINST* **14** (2019) C10043

[9] C. Fanack et al., *Ordinary-mode reflectometry: modification of the scattering and cut-off responses due to the shape of localized density fluctuations, Plasma Phys. Control. Fusion* **38** (1996) 1915

[10] J. Vicente et al., *2D full-wave simulations of conventional reflectometry using 3D gyro-fluid plasma turbulence*, *Plasma Phys. Control. Fusion* **62** (2020) 025031

[11] E. Z. Gusakov et al., *Non-linear theory of fluctuation reflectometry, Plasma Phys. Control. Fusion* **44** (2002) 1565

[12] J. Vicente et al., *Turbulence level effects on conventional reflectometry using 2D full-wave simulations, Rev. Sci. Instrum.* **89** (2018) 10H110